(3+1)-D viscous hydrodynamics CLVisc at finite net baryon density across BES energies

Xiang-Yu Wu

Central China Normal University

In collaboration with Long-Gang Pang, Guang-You Qin and Xin-Nian Wang

13-17 June 2022 Busan, Korea

Outline

- Motivation
- CLVisc hydrodynamics framework
- Numerical results
  - Mean transverse momenta
  - Anisotropic flow
  - Flow fluctuations
- Summary and outlook

Motivation

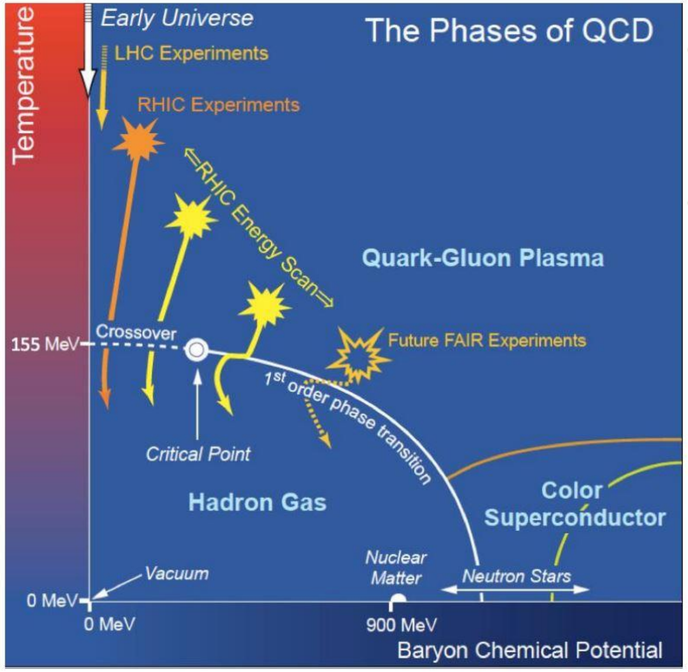

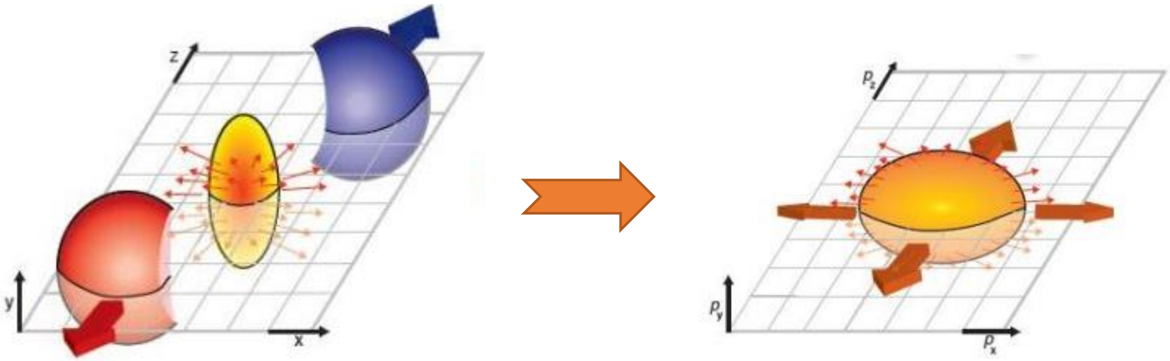

LHC & top RHIC collision energy,
Crossover

Beam energy scan region,
1st order phase transition or
Critical Point

$$\frac{dN}{p_T dp_T dy d\phi} = \frac{dN}{2\pi p_T dp_T dy}\left[1 + 2\sum_n v_n(p_T, y)\cos(n(\phi - \Psi_n(p_T, y)))\right]$$

The collective flow of the QGP fireball converts initial state geometric anisotropy to final state momentum anisotropy.

Hydrodynamics at high collision energy

Hydrodynamics simulation is successful in describing the collective behavior of QGP fireball at zero chemical potential both in transverse plane and longitudinal direction .

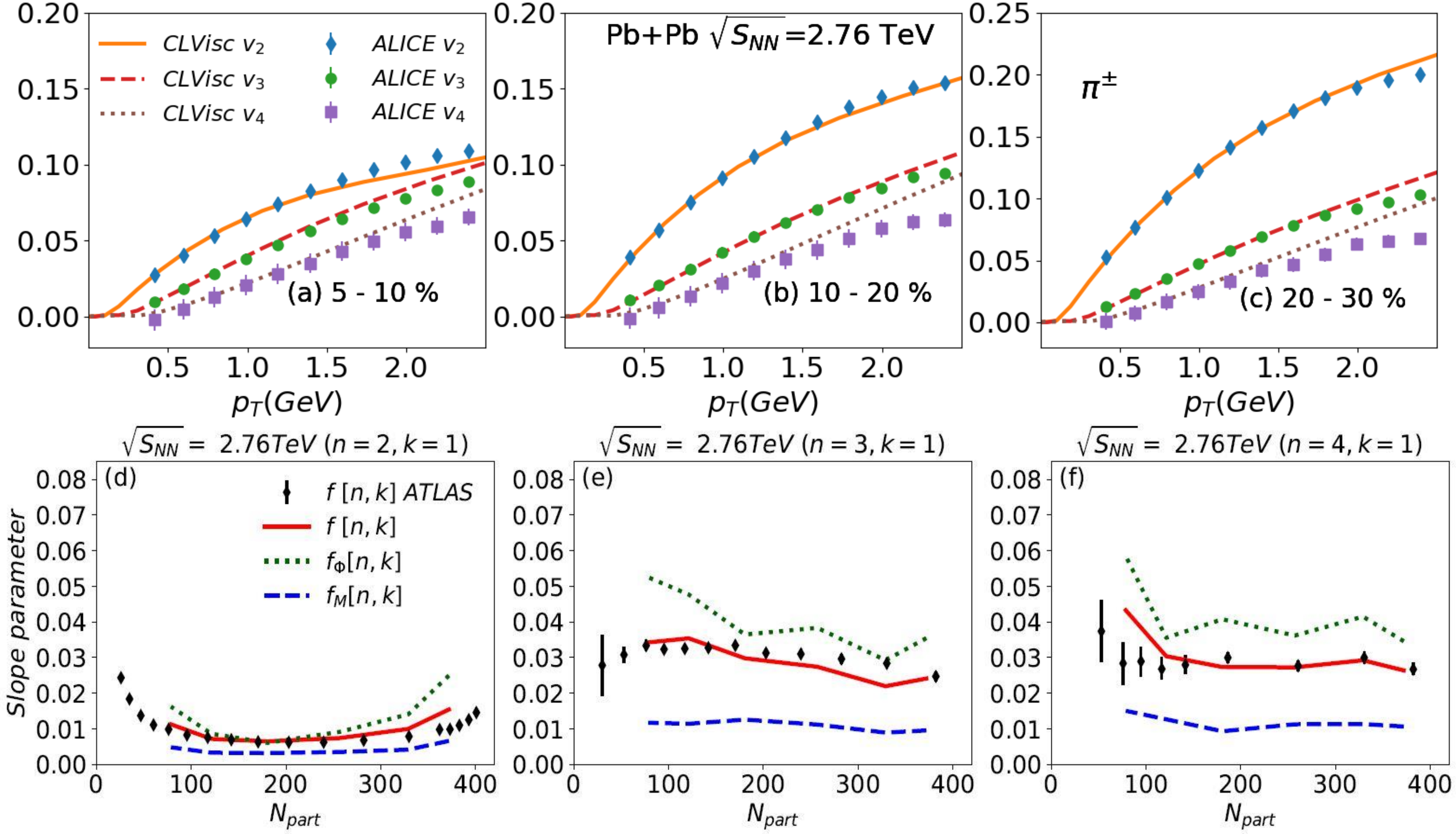

[1] XYW, L.-G. Pang, G.-Y. Qin, and X.-N. Wang, Phys. Rev. C 98, 024913 (2018), arXiv:1805.03762

Hydrodynamics at BES energies

- Constrain the longitudinal dynamics

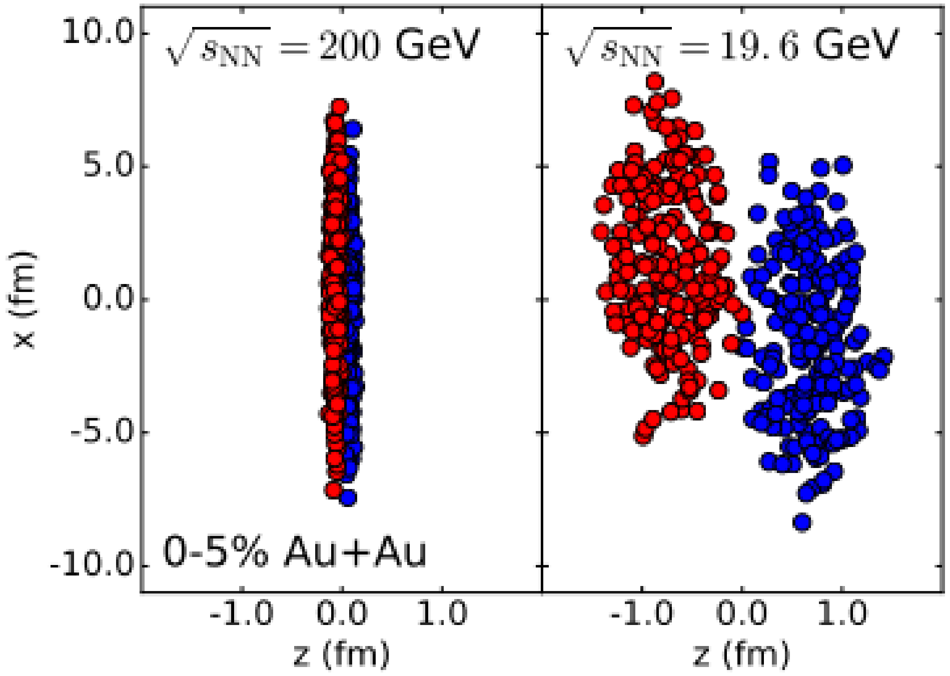

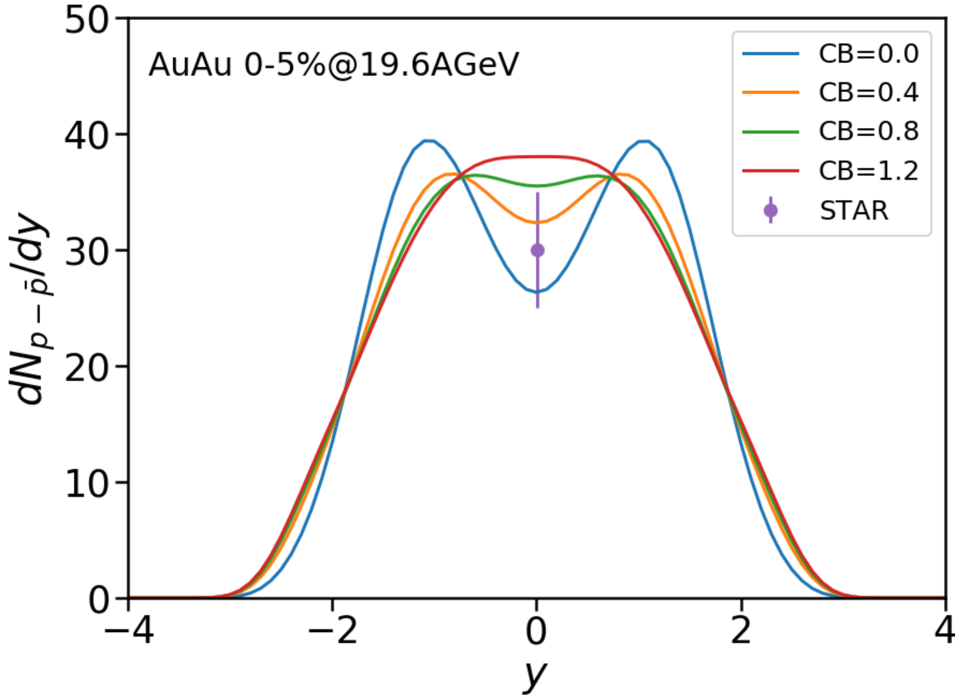

[1] I. A. Karpenko et al, Phys. Rev. C 91, 064901 (2015), arXiv:1502.01978.
[2] G. S. Denicol et al., Phys. Rev. C 98, 034916 (2018), arXiv:1804.10557.
[3] C. Shen and B. Schenke, Phys. Rev. C97, 024907 (2018), arXiv:1710.00881.
[4] L. Du and U. Heinz, Comput. Phys. Commun. 251, 107090 (2020), arXiv:1906.11181.
[5] A. Schafer, I. Karpenko, XYW, J. Hammelmann, and H. Elfner, (2021), arXiv:2112.08724
[6] XYW, G.-Y. Qin, L.-G. Pang, and X.-N. Wang, (2021), arXiv:2107.04949.
[7] C. Shen and B. Schenke, (2022), arXiv:2203.04685.

[Chun Shen's talk@June 14, 10:50 AM]

[Yuuka's talk@June 15, 10:50 AM]

Hydrodynamics at BES energies

- Constrain the longitudinal dynamics
- Vorticity and polarization

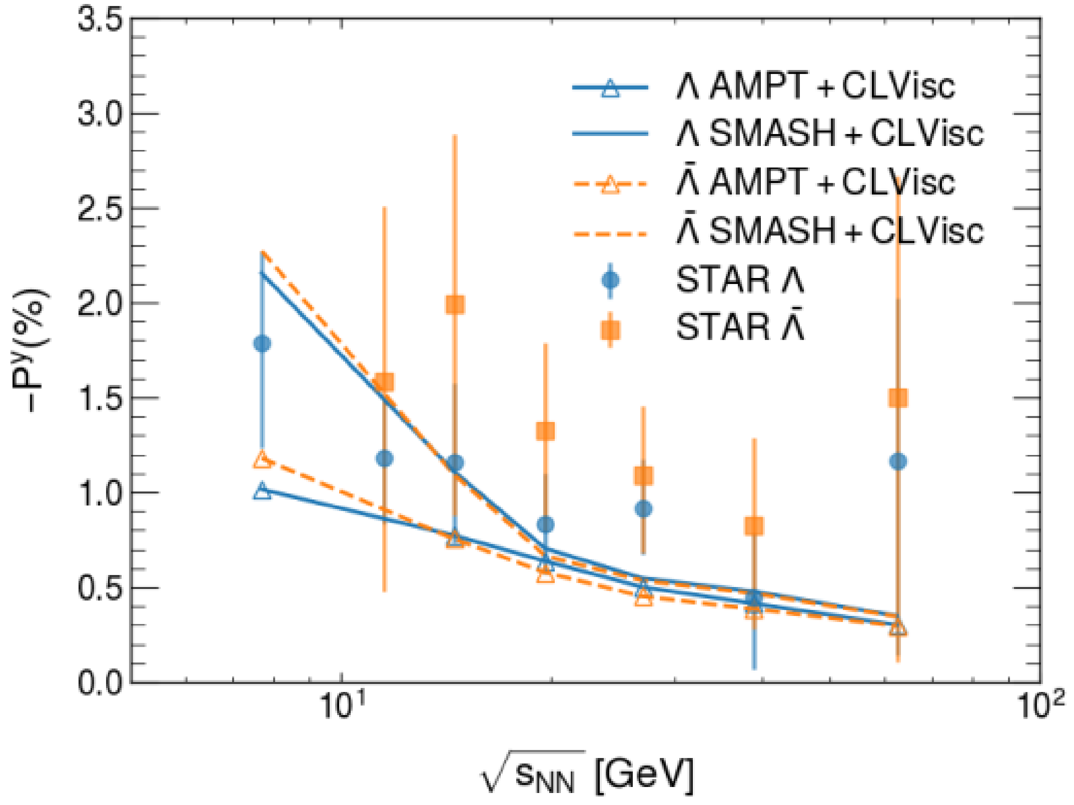

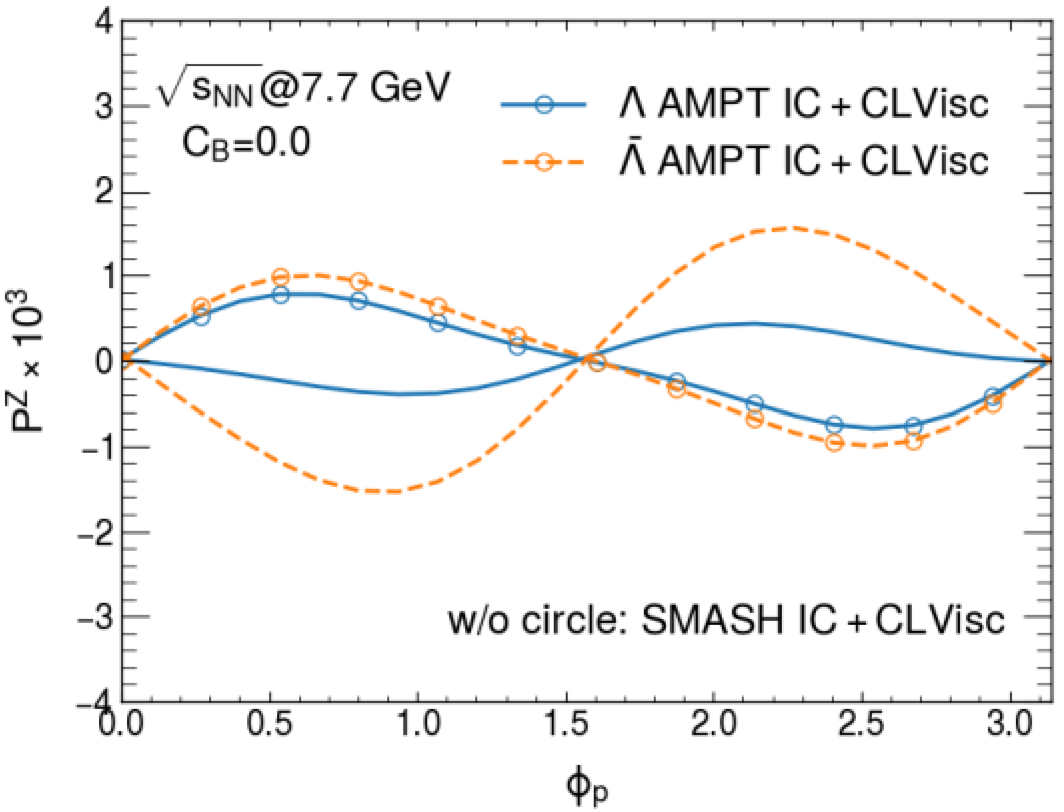

[1] X.-Y. Wu, C. Yi, G.-Y. Qin, and S. Pu, (2022), arXiv:2204.02218

Hydrodynamics at BES energies

- Constrain the longitudinal dynamics
- Vorticity and polarization
- Extract the transport coefficient. $\frac{\eta}{s}(T) \rightarrow \frac{\eta}{s}(T,\mu_B)$, $\frac{\zeta}{s}(T) \rightarrow \frac{\zeta}{s}(T,\mu_B)$

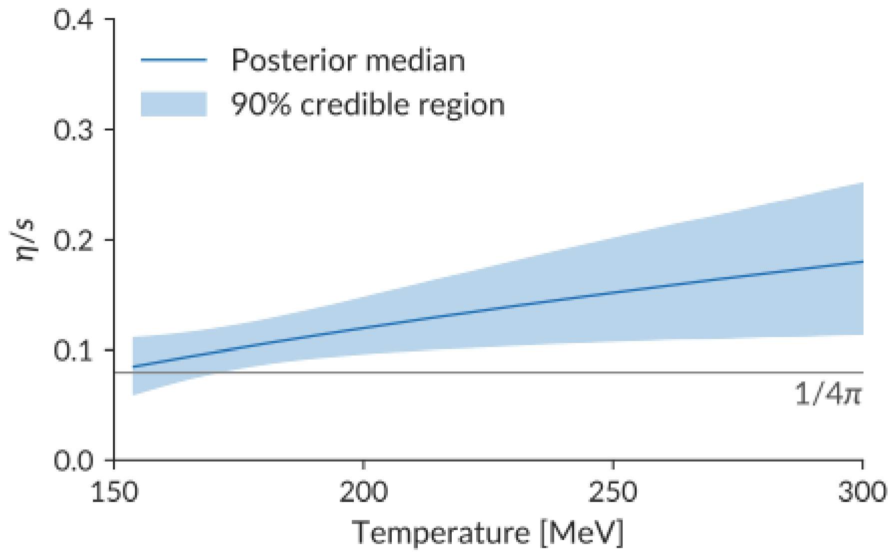

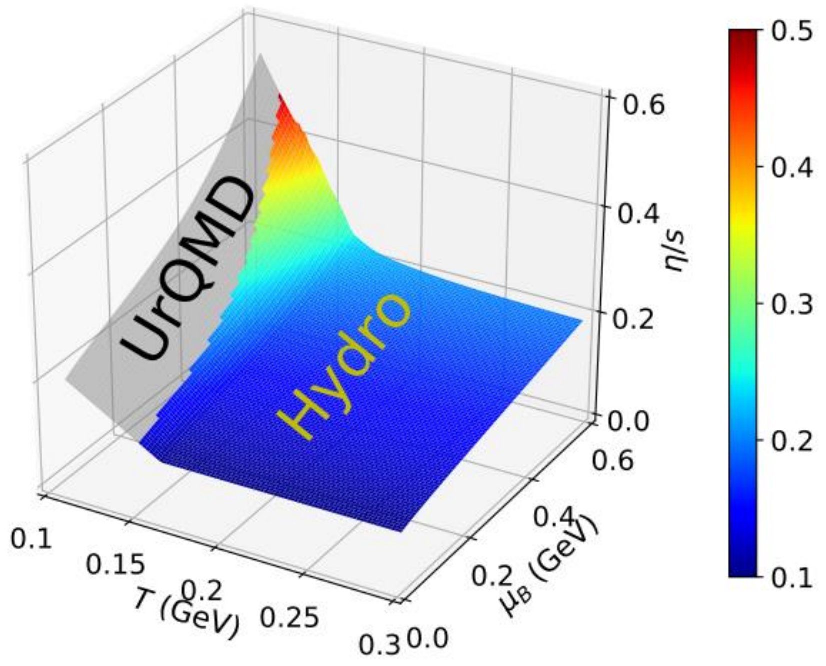

[1] C. Shen and S. Alzhrani, Phys. Rev. C 102, 014909 (2020), arXiv:2003.05852.
[2] J. E. Bernhard, J. S. Moreland, S. A. Bass, J. Liu, and U. Heinz, Phys. Rev. C 94, 024907 (2016), arXiv:1605.03954

Hydrodynamics at BES energies

- Constrain the longitudinal dynamics
- Vorticity and polarization
- Extract the transport coefficient. $\frac{\eta}{s}(T) \rightarrow \frac{\eta}{s}(T,\mu_B)$, $\frac{\zeta}{s}(T) \rightarrow \frac{\zeta}{s}(T,\mu_B)$
- **Hydro+**
- …

Initial States: 3D MC Glauber Model

Local entropy density

$$s(x,y,\eta)|_{\tau_0} = \frac{K}{\tau_0}\left(H_P^s(\eta)\, s_p(x,y) + H_T^s\, s_T(x,y)\right)$$

Local baryon density

$$n(x,y,\eta)|_{\tau_0} = \frac{1}{\tau_0}\left(H_P^n(\eta)\, s_p(x,y) + H_T^n\, s_T(x,y)\right)$$

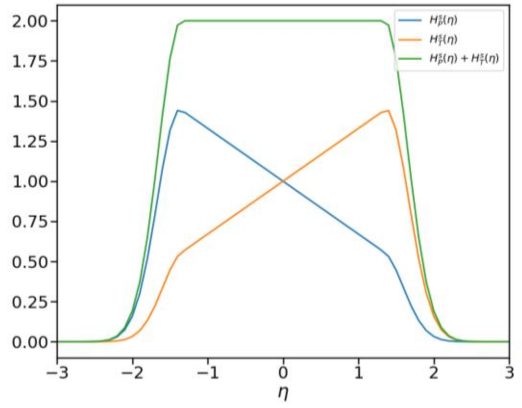

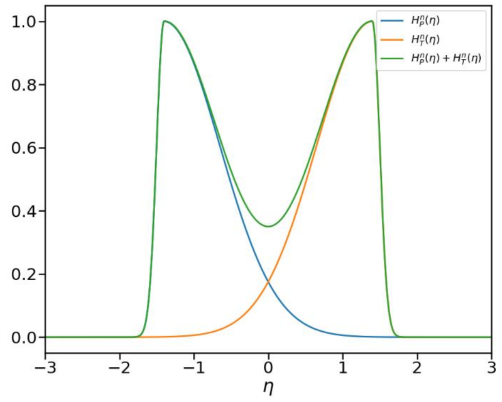

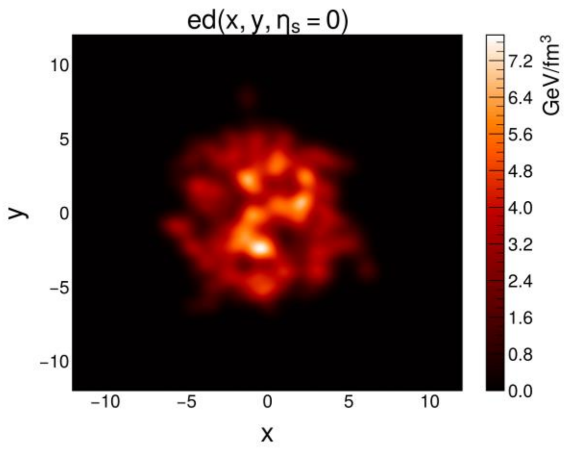

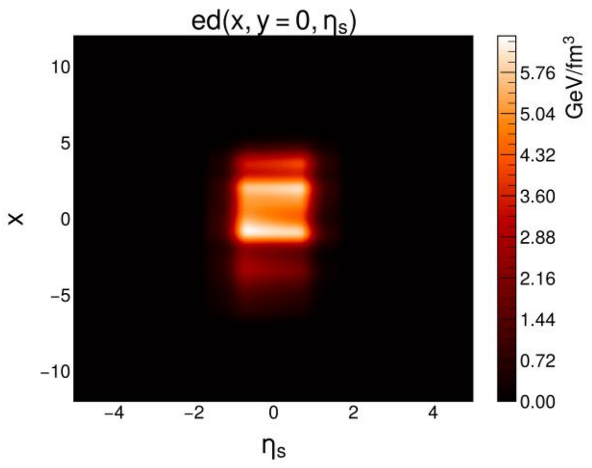

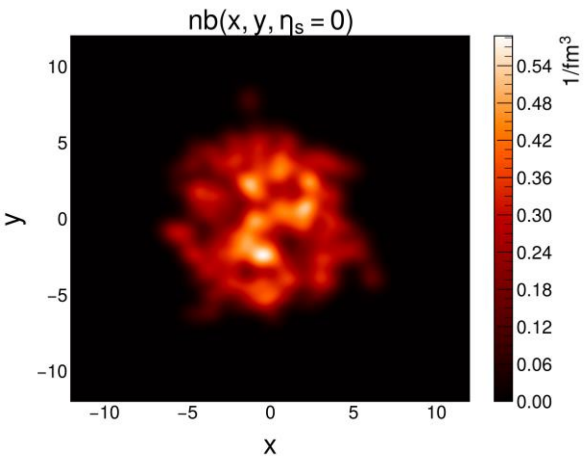

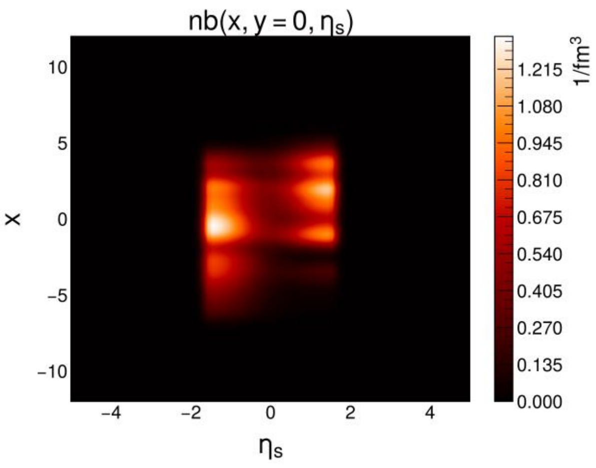

Hydrodynamical Evolution

Energy – momentum conservation and net baryon current conservation:

$$\partial_\mu T^{\mu\nu} = 0 \qquad T^{\mu\nu} = eU^\mu U^\nu - (P+\Pi)\Delta^{\mu\nu} + \pi^{\mu\nu}$$

$$\partial_\mu J^\mu = 0 \qquad J^\mu = nU^\mu + V^\mu$$

Equation of motion of dissipative current:

$$\Delta^{\mu\nu}_{\alpha\beta} D\pi^{\alpha\beta} = -\frac{1}{\tau_\pi}(\pi^{\mu\nu} - \eta\sigma^{\mu\nu}) - \frac{4}{3}\pi^{\mu\nu}\theta - \frac{5}{7}\pi^{\alpha\langle\mu}\sigma^{\nu\rangle}_{\alpha} + \frac{9}{70}\frac{4}{e+P}\pi^{\langle\mu}_{\alpha}\pi^{\nu\rangle\alpha}$$

$$\Delta^{\mu\nu} DV_\mu = -\frac{1}{\tau_V}\left(V^\mu - \kappa_B \nabla^\mu \frac{\mu}{T}\right) - V^\mu\theta - \frac{3}{10}V_\nu\sigma^{\mu\nu}$$

The shear viscosity

$$\eta = C_\eta \frac{e+P}{T}$$

The baryon diffusion

$$\kappa_B = \frac{C_B}{T} n\left(\frac{1}{3}\cot\left(\frac{\mu_B}{T}\right) - \frac{nT}{e+P}\right)$$

Equation of state P(e, n): NEOS (Lattice QCD + hadron gas, crossover)

[1] G. S. Denicol et al., Phys. Rev. C 98, 034916 (2018), arXiv:1804.10557.
[2]Monnai, Akihiko et al. Phys.Rev. C100 (2019) no.2, 024907 arXiv:1902.05095 [nucl-th]

Particlization and Afterburner

Cooper-Frye Formula

$$\frac{dN}{dYp_T dp_T d\phi} = \frac{g_i}{(2\pi)^3}\int_\Sigma p^\mu d\Sigma_\mu f^{\mathrm{eq}}(1+\delta f_\pi + \delta f_V)$$

Out-of-equilibrium corrections

$$\delta f_\pi(x,p) = (1 \pm f^{\mathrm{eq}}(x,p))\frac{p_\mu p_\nu \pi^{\mu\nu}}{2T_f^2(e+P)} \qquad \delta f_V(x,p) = (1 \pm f^{\mathrm{eq}}(x,p))\left(\frac{n}{e+P} - \frac{B}{U^\mu p_\mu}\right)\frac{p^\mu V_\mu}{\kappa_B/\tau_V}$$

SMASH 1.8: a novel and modern hadronic transport approach

$$p^\mu \partial_\mu f + mF^\mu \partial_{p_\mu} f = C[f]$$

C[f]: elastic collisions, resonance formation and decays, string fragmentation for all mesons and baryons up to mass ~ 2.35 GeV

[1] G. S. Denicol et al., Phys. Rev. C 98, 034916 (2018), arXiv:1804.10557.
[2] J. Weil et al., Phys. Rev. C 94, 054905 (2016), arXiv:1606.06642

Mean transverse Momenta

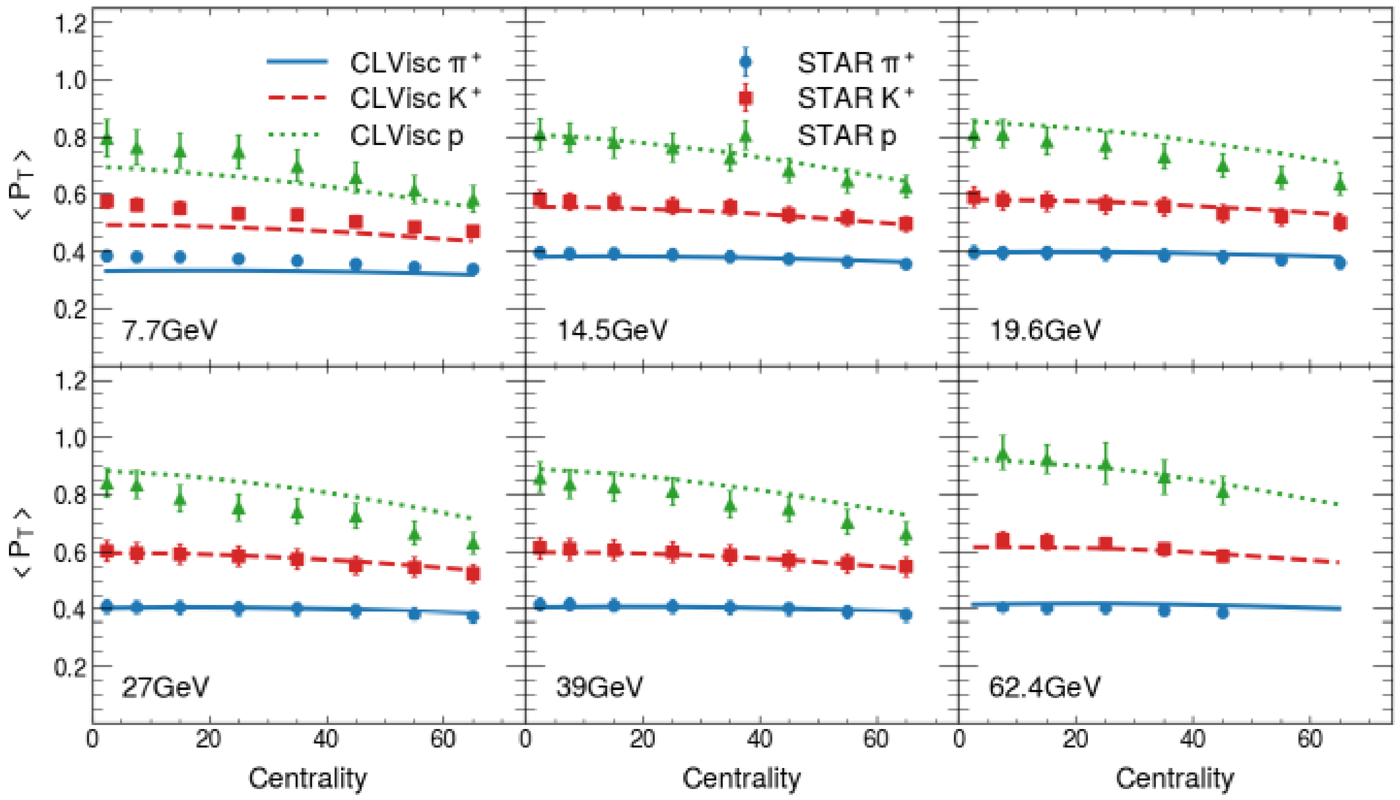

The CLVisc framework can describe mean transverse momenta of identified particles from STAR .

One can clearly see more blue shift effect for more massive particles

Mean transverse Momenta

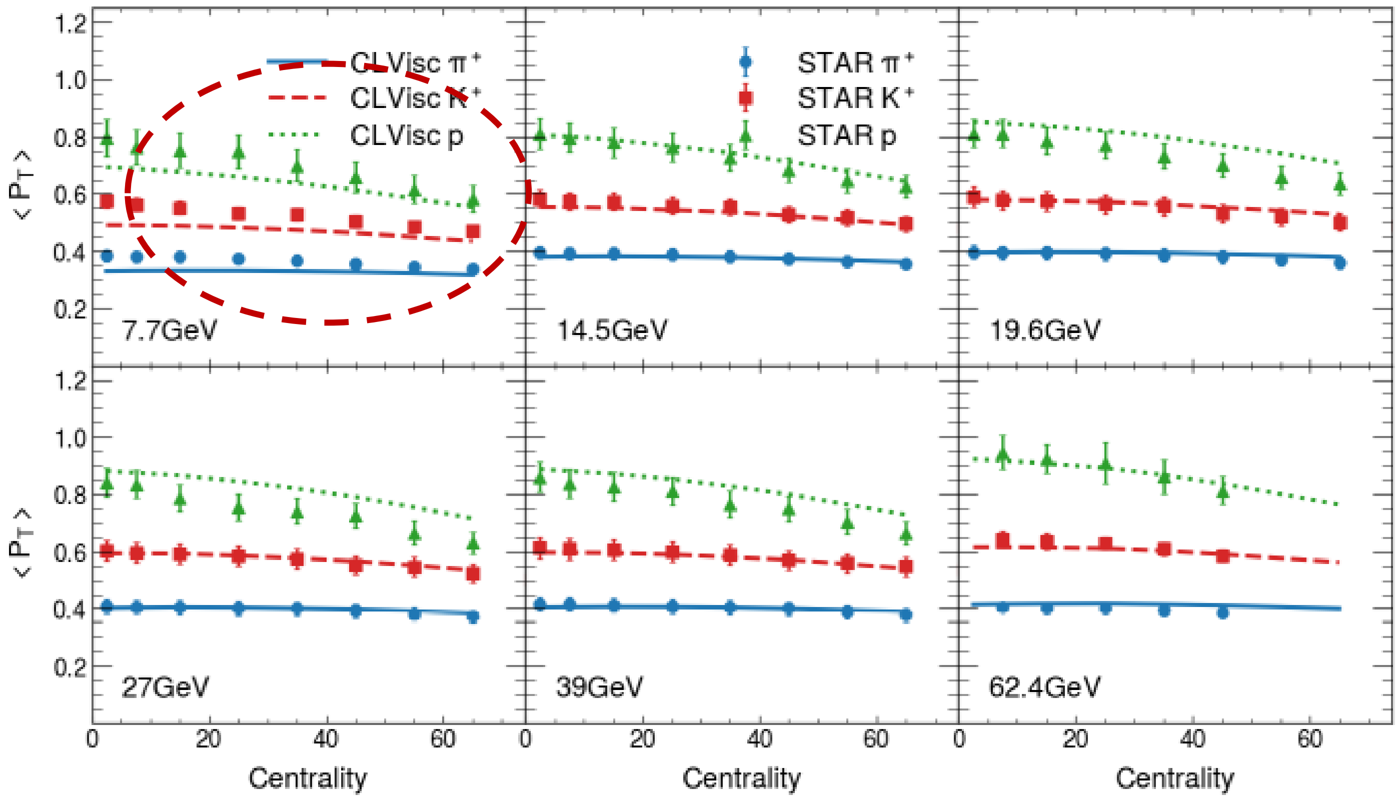

The CLVisc framework can describe mean transverse momenta of identified particles from STAR .

One can clearly see more blue shift effect for more massive particles

The initial conditions and pre-equilibrium evolution should improve the model in the future.

Mean transverse Momenta

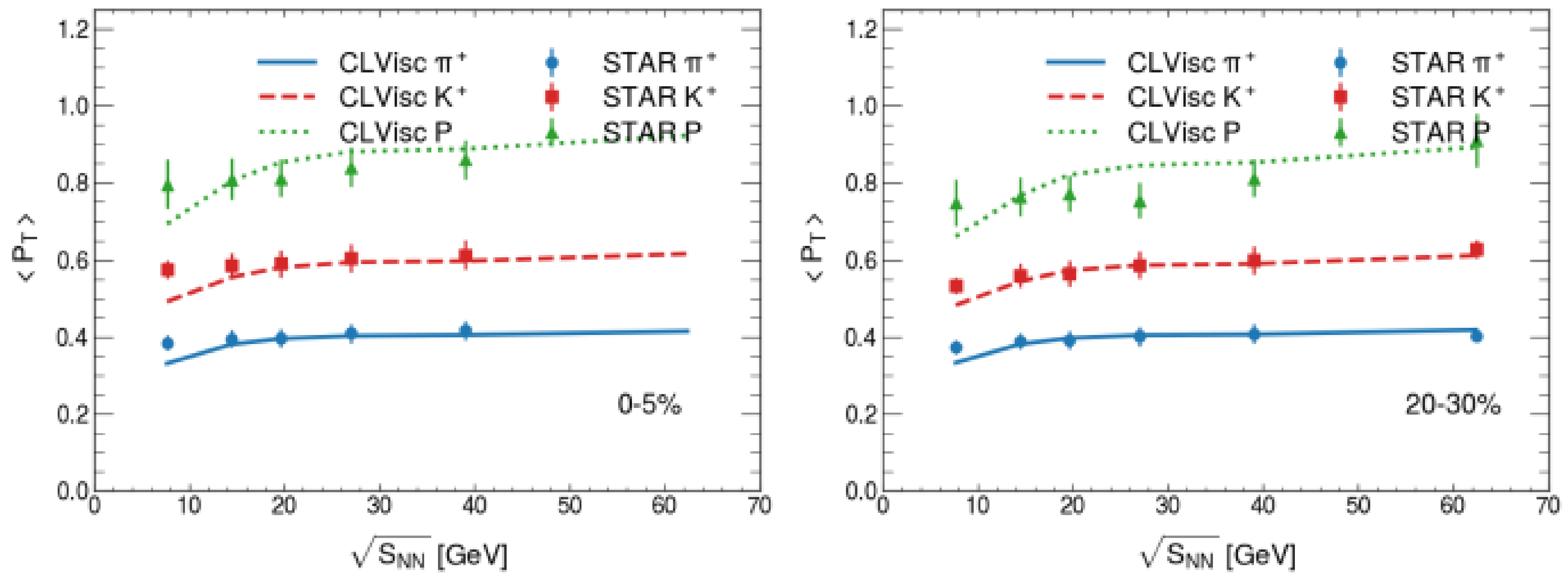

One can clearly see more blue shift effect for more massive particles

The mean momenta of π^+, K^+ and P increase mildly with the collision energy due to larger radial flow.

Anisotropic flows

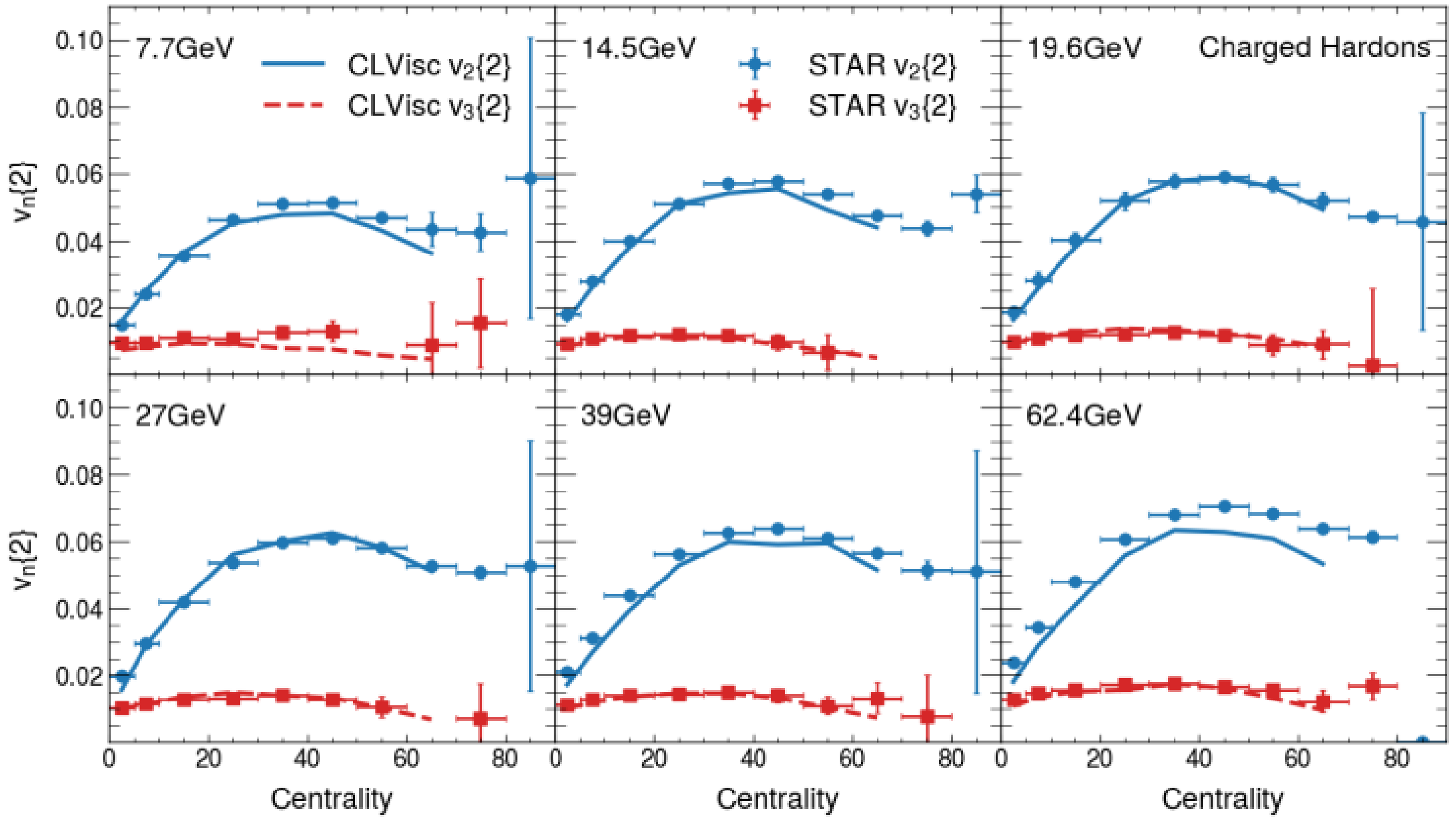

Our results are in good agreement with the experimental data from STAR:

- $v_2\{2\}$: typical non-monotonic centrality dependences due to the combined effect of the elliptic geometry, geometrical fluctuations and the system size.
- $v_3\{2\}$: weak centrality dependence due to the initial state geometrical fluctuations.

Anisotropic flows

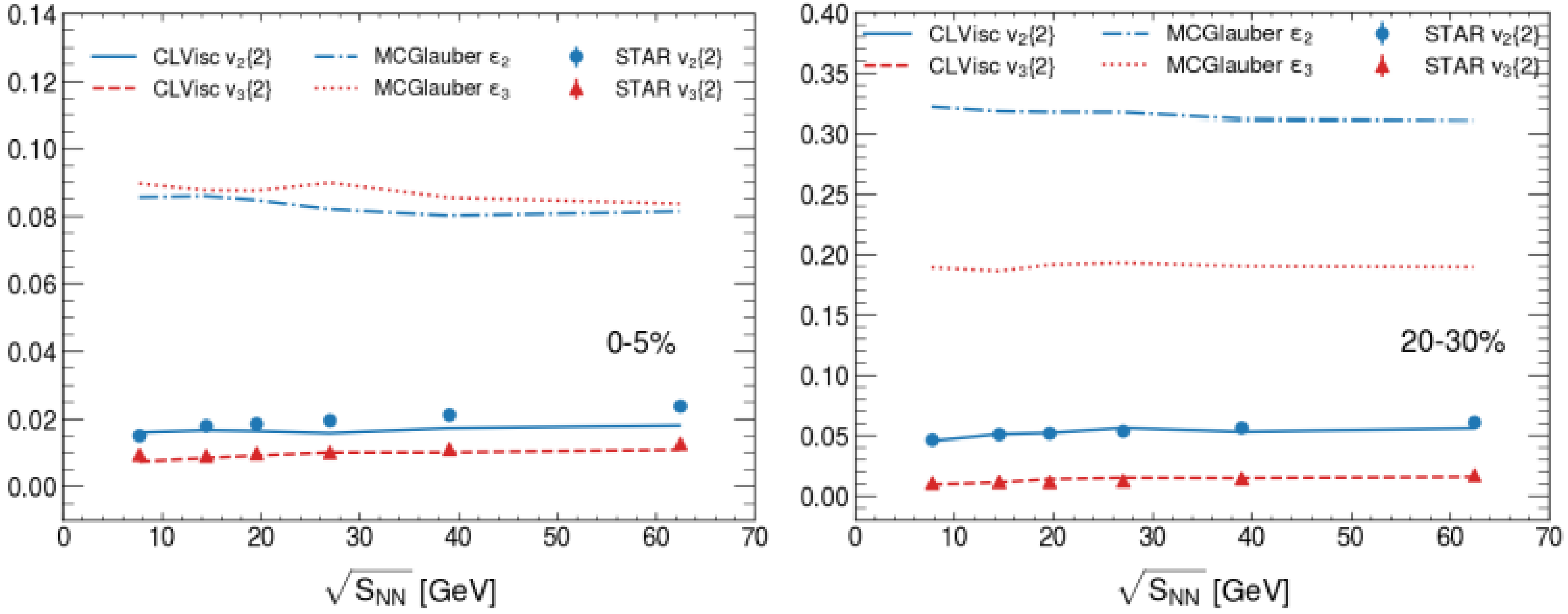

We find that both elliptic and triangular flows increase slightly with the beam energy.

- the eccentricities ε_2 and ε_3 have very weak dependence on collision energy
- the increase of radial flow due to the increase of initial energy density

Flows fluctuations

STAR, M. Abdallah et al., (2022), arXiv:2201.10365

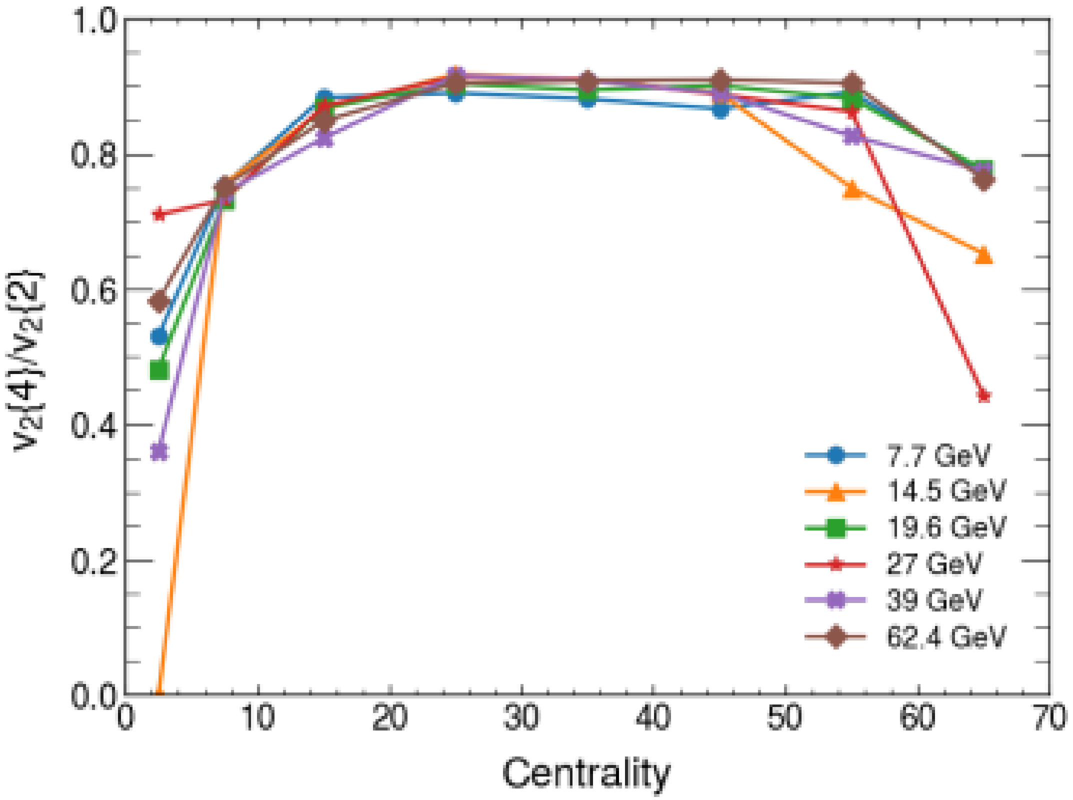

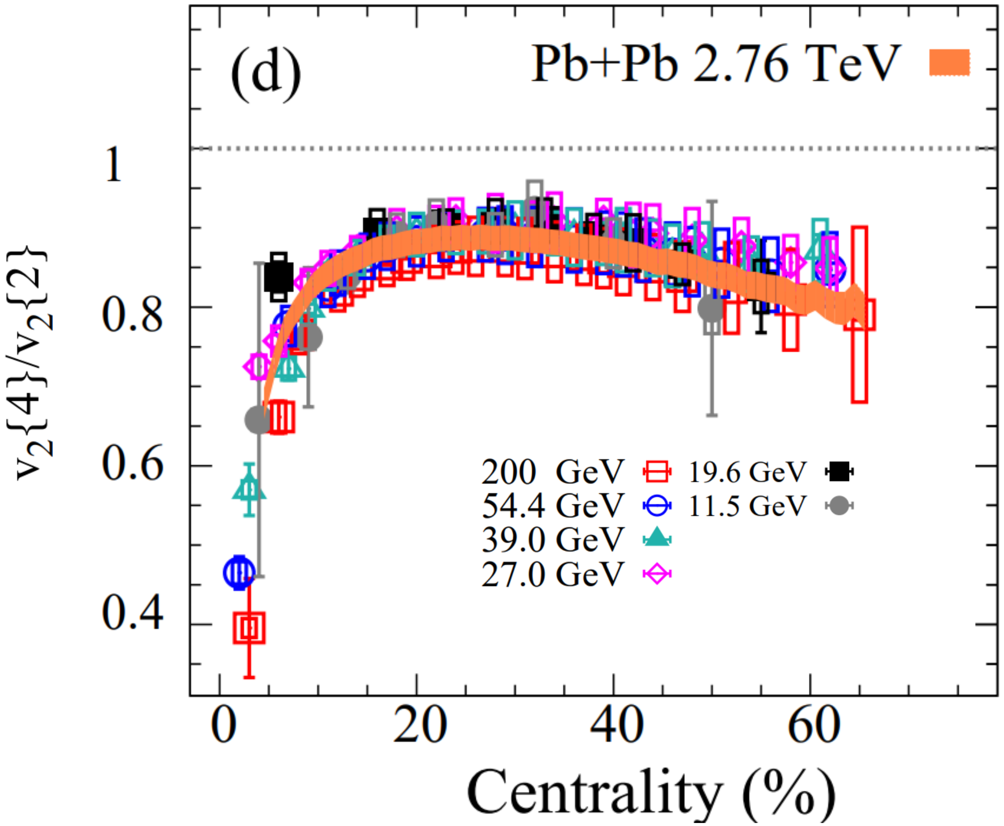

The multi-particle cumulant ratio $v_2\{4\}/v_2\{2\}$ first increases, and then decreases with centrality increased.

- initial collision geometry dominates in mid-central collisions.
- the fluctuations dominate in central and peripheral collisions.

The multi-particle cumulant ratio $v_2\{4\}/v_2\{2\}$ has weak collision energy dependence

Summary

We developed the (3+1)-D CLVisc hydrodynamic framework to include fluctuation initial condition, 2nd viscous hydrodynamics with baryon charge using the equation of state from NEOS, and hadronic transport SMASH afterburner.

Our calculation provides a benchmark for understanding the RHIC-BES data.

Elliptic and triangular flows increase slightly with the beam energy.

The multi-particle cumulant ratio $v_2\{4\}/v_2\{2\}$ has weak collision energy dependence.

Outlook

Hydro+, critical fluctuations

Back Up

CLVisc at non-zero μ_B

Initial condition: MC Glauber model

Local entropy density

$$s(x,y,\eta)|_{\tau_0} = \frac{K}{\tau_0}\left(H_P^s(\eta)s_p(x,y) + H_T^s(\eta)s_T(x,y)\right)$$

Local baryon density

$$n(x,y,\eta)|_{\tau_0} = \frac{1}{\tau_0}\left(H_P^n(\eta)s_p(x,y) + H_T^n(\eta)s_T(x,y)\right)$$

where

$$s_{P/T}(x,y) = \sum_{i=1}^{N_{\text{part}}^{P/T}} \frac{1}{2\pi\sigma_r^2}\exp\left(-\frac{(x-x_i)^2+(y-y_i)^2}{2\pi\sigma_r^2}\right) \quad , \quad \tau_0 = \tau_{\text{overlap}} = \frac{2R}{\sqrt{\gamma^2-1}}$$

Longitudinal profile

$$H_{P/T}^s = \theta(\eta_{\max}-|\eta|)\left(1 \pm \frac{\eta}{y_{\text{beam}}}\right)\left[\theta(|\eta|-\eta_0^s)\exp\left(-\frac{(|\eta|-\eta_0^s)^2}{2\sigma_s^2}\right) + \theta(\eta_0^s-|\eta|)\right]$$

$$H_{P/T}^n = \frac{1}{N}\left[\theta(\eta-\eta_0^{n,P/T})\exp\left(-\frac{(\eta-\eta_0^{n,P/T})^2}{2\sigma_{P/T}^2}\right) + \theta(\eta_0^{n,P/T}-\eta)\exp\left(-\frac{(\eta-\eta_0^{n,P/T})^2}{2\sigma_{T/P}^2}\right)\right]$$

Denicol, Gabriel S. *et al.* Phys.Rev. C98 (2018) no.3, 034916 arXiv:1804.10557 [nucl-th]

Set-up

$\sqrt{s_{NN}}$ [GeV]	K	τ_0 [fm]	σ_s [fm]	η_0^s	$\sigma_{n;P}$	$\sigma_{n;T}$	$\eta_{0;P/T}^n$
7.7	7.67	3.6	0.3	0.9	0.07	0.7	1.05
14.5	9.22	2.2	0.3	1.15	0.14	0.81	1.4
19.6	10.22	1.8	0.3	1.3	0.14	0.85	1.5
27	10.35	1.4	0.3	1.6	0.14	1.06	1.8
39	10.35	1.3	0.3	1.9	0.14	1.13	2.2
62.4	10.8	1.0	0.3	2.25	0.14	1.34	2.7

TABLE I: The parameters for a 3-dimensional Monte-Carlo Glauber model for initial conditions.

Shear viscosity C_η = 0.08
Baryon diffusion coefficient , C_B = 0.4
Freezeout energy density Efrz = 0.4 GeV/fm^3

Regulation:

$$\max(|\pi^{\mu\nu}|) > T_{\text{ideal}}^{\tau\tau} \quad \Rightarrow \quad \pi^{\mu\nu} = 0$$

$$\max(|V^{\mu}|) > J_{\text{ideal}}^{\tau} \quad \Rightarrow \quad V^{\mu} = 0$$

We use a step function $\theta(f_{\text{eq}} + \delta f_\pi + \delta f_V)$ so that the full (equilibrium and nonequilibrium) distribution functions never encounter negative values. (PTM and the maximum-entropy distribution)

The modified Cooper-Frye formula

$$\mathcal{S}^{\mu}(\mathbf{p}) = \frac{\int d\Sigma \cdot p\mathcal{J}_5^{\mu}(p,X)}{2m\int d\Sigma \cdot \mathcal{N}(p,X)}$$

$\mathcal{J}_5^{\mu}(p,X)$: axial-charge current density

$\mathcal{N}(p,X)$: the number density of fermions

From quantum kinetic theory

$$\mathcal{S}^{\mu}(\mathbf{p}) = \mathcal{S}^{\mu}_{\text{thermal}}(\mathbf{p}) + \mathcal{S}^{\mu}_{\text{shear}}(\mathbf{p}) + \mathcal{S}^{\mu}_{\text{ace T}}(\mathbf{p}) + \mathcal{S}^{\mu}_{\text{chemical}}(\mathbf{p}) + \mathcal{S}^{\mu}_{\text{EB}}(\mathbf{p})$$

$$\mathcal{S}^{\mu}_{\text{thermal}}(\mathbf{p}) = \int d\Sigma^{\sigma} F_{\sigma}\epsilon^{\mu\nu\alpha\beta} p_{\nu}\partial_{\alpha}\frac{u_{\beta}}{T}$$

$$\mathcal{S}^{\mu}_{\text{shear}}(\mathbf{p}) = \int d\Sigma^{\sigma} F_{\sigma}\frac{\epsilon^{\mu\nu\alpha\beta} p_{\nu} u_{\beta}}{(u\cdot p)T} \times p^{\rho}(\partial_{\rho}u_{\alpha} + \partial_{\alpha}u_{\rho} - u_{\rho}Du_{\alpha})$$

$$\mathcal{S}^{\mu}_{\text{accT}}(\mathbf{p}) = -\int d\Sigma^{\sigma} F_{\sigma}\frac{\epsilon^{\mu\nu\alpha\beta} p_{\nu} u_{\alpha}}{T}\left(Du_{\beta} - \frac{\partial_{\beta}T}{T}\right)$$

$$\mathcal{S}^{\mu}_{\text{chemical}}(\mathbf{p}) = 2\int d\Sigma^{\sigma} F_{\sigma}\frac{1}{(u\cdot p)}\epsilon^{\mu\nu\alpha\beta} p_{\alpha} u_{\beta}\partial_{\nu}\frac{\mu}{T}$$

$$\mathcal{S}^{\mu}_{\text{EB}}(\mathbf{p}) = 2\int d\Sigma^{\sigma} F_{\sigma}\left[\frac{\epsilon^{\mu\nu\alpha\beta} p_{\alpha} u_{\beta} E_{\nu}}{(u\cdot p)T} + \frac{B^{\mu}}{T}\right]$$

$$F^{\mu} = \frac{\hbar}{8m_{\Lambda}\Phi(\mathbf{p})} p^{\mu} f_{eq}(1 - f_{eq})$$

$$\Phi(\mathbf{p}) = \int d\Sigma^{\mu} p_{\mu} f_{eq}$$

CLVisc Hydrodynamics Framework

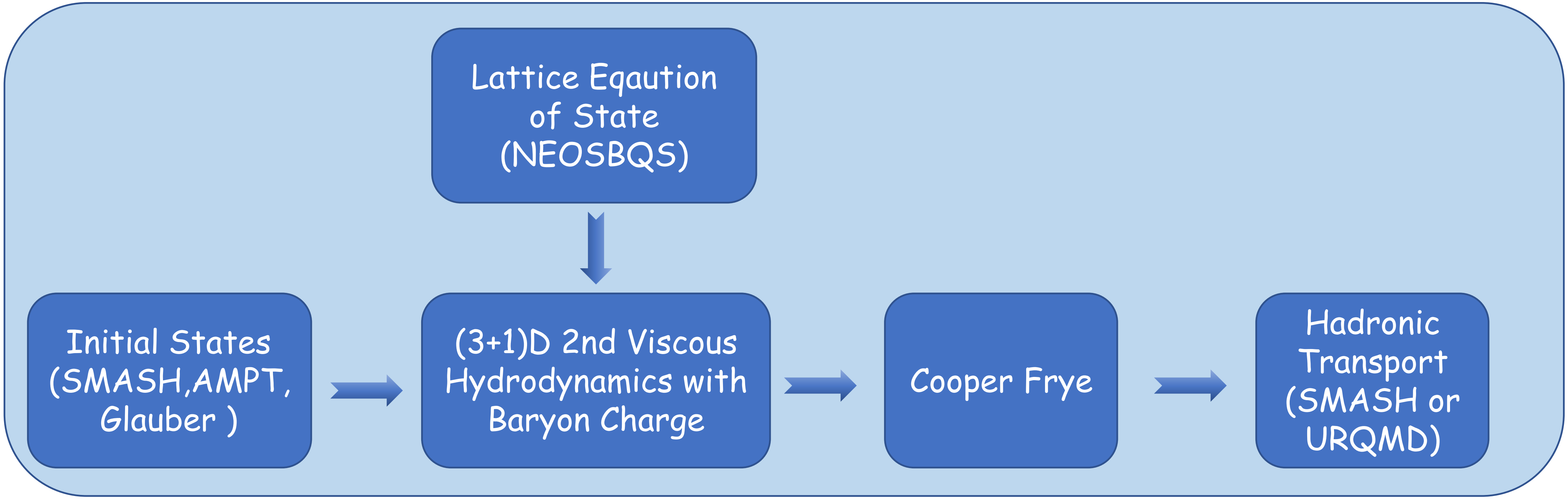

Transverse: Gubser flow

To test the numerical accuracy of new CLVisc code, we compare our numerical results with both analytical solutions of the hydrodynamic equations and other independent codes.

Gubser flow: strong radial flow, longitudinal invariance in conformal system.

$$\varepsilon(\tau,r) = \frac{\varepsilon}{\tau^4}\frac{(2q\tau)^{\frac{8}{3}}}{\left[1+2q^2(\tau^2+r^2)+q^4(\tau^2-r^2)^2\right]^{\frac{4}{3}}}$$

$$n(\tau,r) = \frac{n_0}{\tau^4}\frac{(2q\tau)^2}{\left[1+2q^2(\tau^2+r^2)+q^4(\tau^2-r^2)^2\right]}$$

with $v_\perp(\tau,r) = \dfrac{2q^2\tau r}{1+(q\tau)^2+(qr)^2}$

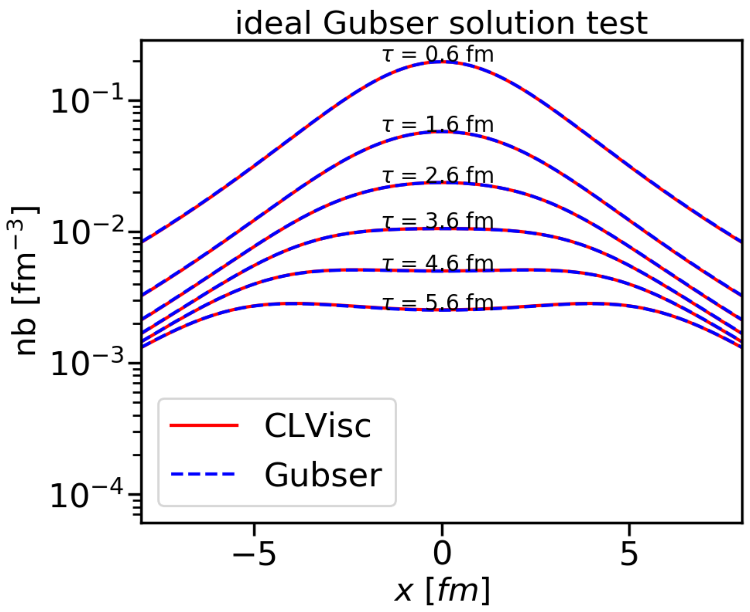

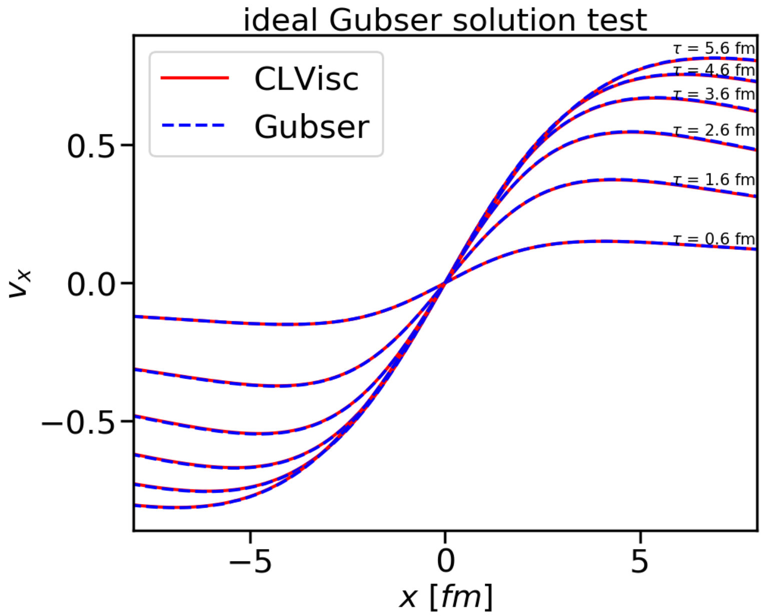

Longitudinal: (1+1)D Monnai's code

In longitudinal direction, we compare between the CLVisc's numerical results and (1+1) D hydrodynamic code by Monnai.

$$\Delta^{\mu\nu} D V_{\mu} = -\frac{1}{\tau_{V}}\left(V^{\mu} - \kappa_B \nabla^{\mu}\frac{\mu}{T}\right)$$

where $\kappa_B = \dfrac{0.2n}{\mu_B}$ $\quad \tau_V = \dfrac{0.2}{T}$

Denicol, Gabriel S. *et al.* Phys.Rev. C98 (2018) no.3, 034916 arXiv:1804.10557 [nucl-th]
Monnai, Akihiko Phys.Rev. C86 (2012) 014908 arXiv:1204.4713 [nucl-th]

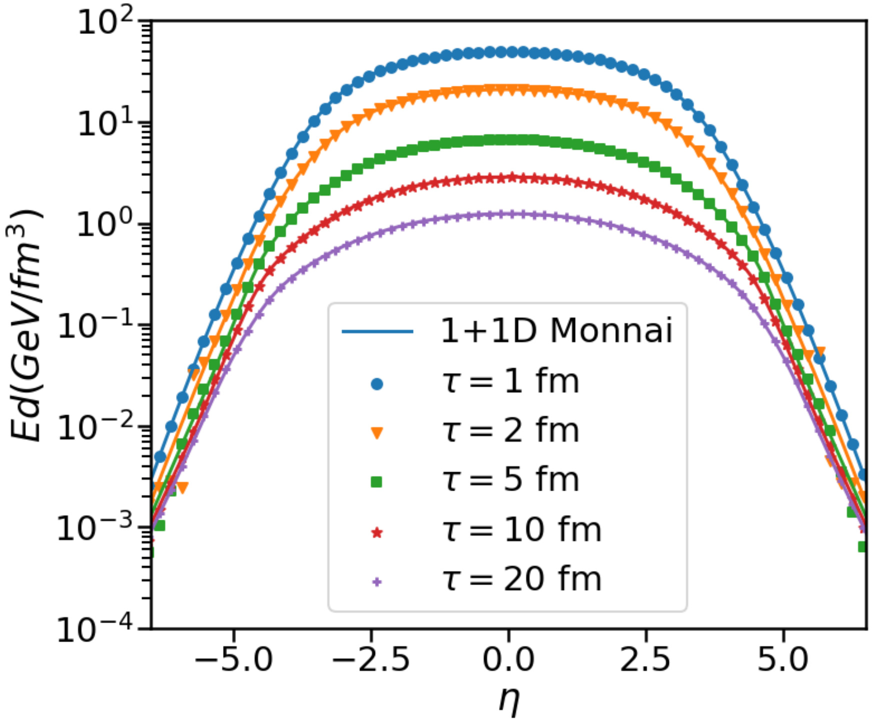

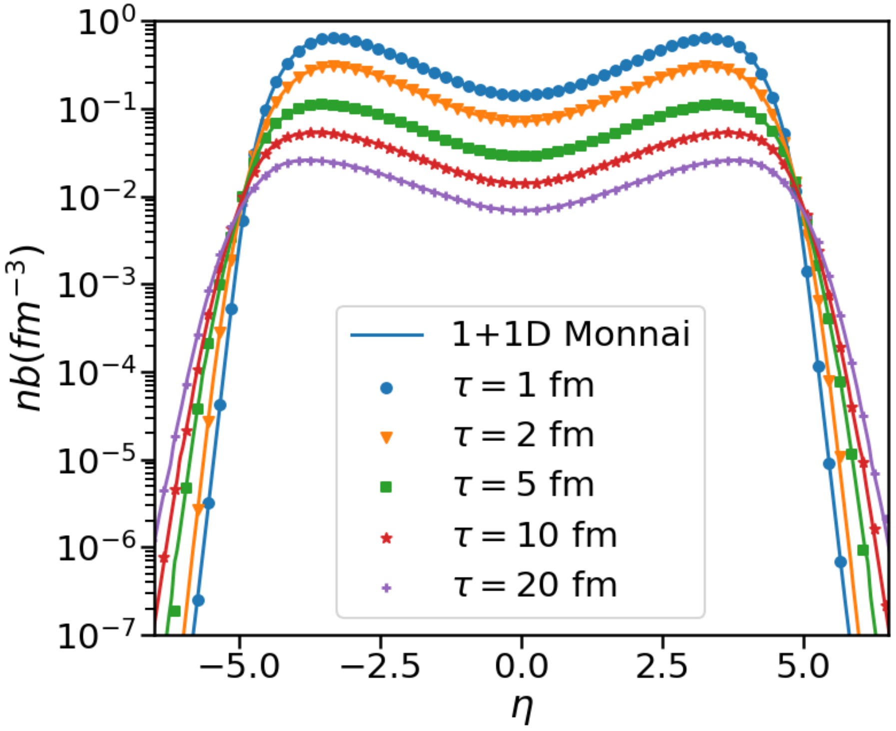

Compared with VHLLE hydro model

VHLLE: a (3+1) D hydrodynamics model developed by Iurii Karpenko